

# Exemplar-condensed Federated Class-incremental Learning

Rui Sun, Yumin Zhang, Varun Ojha, Tejal Shah, Haoran Duan, Bo Wei, Rajiv Ranjan

School of Computing, Newcastle University, UK

{Rui.Sun, Y.Zhang361, Varun.Ojha, Tejal.Shah, Haoran.Duan, Bo.Wei, Rajiv.Ranjan}@newcastle.ac.uk

## Abstract

We propose **Exemplar-Condensed federated class-incremental learning (ECoral)** to distill the training characteristics of real images from streaming data into informative rehearsal exemplars. The proposed method eliminates the limitations of exemplar selection in replay-based approaches for mitigating catastrophic forgetting in federated continual learning (FCL). The limitations particularly related to the heterogeneity of information density of each summarized data. Our approach maintains the consistency of training gradients and the relationship to past tasks for the summarized exemplars to represent the streaming data compared to the original images effectively. Additionally, our approach reduces the information-level heterogeneity of the summarized data by inter-client sharing of the disentanglement generative model. Extensive experiments show that our ECoral outperforms several state-of-the-art methods and can be seamlessly integrated with many existing approaches to enhance performance.

## Introduction

Federated Learning (FL) (McMahan et al. 2017) enables the collaborative training of a global model across thousands of clients while keeping data decentralized. It effectively addresses the challenges presented by data silos, facilitating a cooperative learning environment without compromising individual privacy, and has been applied in various areas such as smart healthcare (Nguyen et al. 2022) and Internet-of-Things applications (Nguyen et al. 2021; Jiang et al. 2024). However, traditional FL methods assume the application scenario is static, which conflicts with the realistic environment where the data of novel classes can emerge at any time (Yoon et al. 2021; Ma et al. 2022). Simply fine-tuning the pre-trained model to the novel data results in *catastrophic forgetting* (Li and Hoiem 2017), where the model’s performance significantly deteriorates on previously learned tasks. Moreover, the constraints of limited computational resources and data privacy concerns, which allow only a limited selection of previously learned data to be stored, make retraining a model from scratch impractical.

To address these challenges, recent work (Dong et al. 2022, 2024; Zhang et al. 2023) has enabled the FL frame-

Copyright © 2025, Association for the Advancement of Artificial Intelligence (www.aaai.org). All rights reserved.

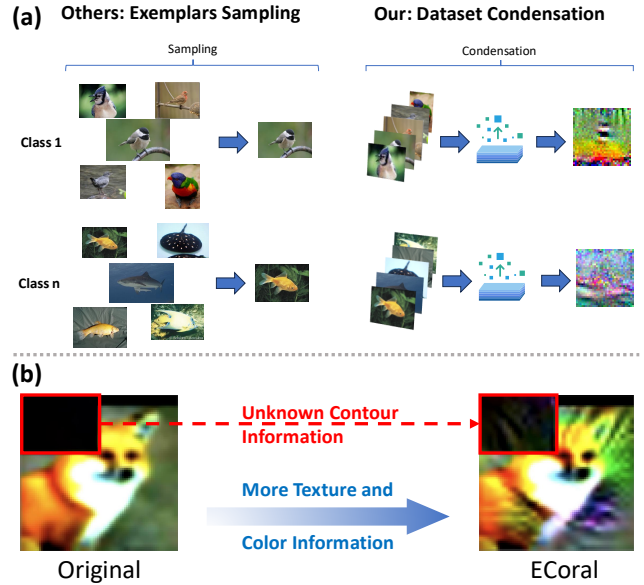


Figure 1: Comparison between our approach and others. (a) Most Federated Continual Learning (FCL) methods use exemplars sampled from training data, whereas our method, ECoral, extracts and summarizes more comprehensive information, producing more informative exemplars. (b) ECoral can capture hidden contour information and enrich class-specific features such as texture and color, making the exemplars more representative of the overall data.

work to incrementally learn novel classes, known as Federated Class-Incremental Learning (FCIL). Among various strategies proposed for FCIL, rehearsal-based methods (Dong et al. 2022; Qi, Zhao, and Li 2023) that store and replay exemplars from prior tasks stand out as effective approaches in mitigating the forgetting problem. However, these methods are limited by the constrained storage resources of edge devices and privacy concerns, allowing only a limited selection of data. This raises a crucial **question**: *How can a restricted dataset be utilized to encapsulate more information and effectively counteract the forgetting problem without compromising data privacy?*

A straightforward approach involves directly compress-

ing data into a compact format. While this method efficiently condenses information, it is not necessarily ideal for training machine learning models. Even over-compression can lead to excessively complex information, hindering the model’s ability to distinguish decision boundaries effectively. Data condensation (DC) (Wang et al. 2018; Zhao, Mopuri, and Bilen 2020) has emerged as a prominent solution that employs sophisticated approaches, such as distribution/feature matching (Wang et al. 2022; Zhao and Bilen 2023) or gradient/trajectory matching surrogate objectives (Zhao, Mopuri, and Bilen 2020; Cazenavette et al. 2022), to synthesize compact datasets. These condensed datasets are meticulously crafted to encapsulate the quintessential characteristics of the original, larger datasets. These condensed datasets are carefully crafted to capture the core characteristics of larger datasets and enable models trained on them to achieve performance comparable to those trained on the full datasets.

Most recently, several works (Goetz and Tewari 2020; Hu et al. 2022; Liu, Yu, and Zhou 2022; Xiong et al. 2023) have introduced DC into the FL framework, replacing the traditional exchange of model parameters with only a small portion of synthetic data. In contrast, in this work, we focus on leveraging DC to improve exemplar replay efficiency by maximizing the information stored in condensed datasets, thus better mitigating catastrophic forgetting. However, simply implementing such methods (Masarczyk and Tautkute 2020; Rosasco et al. 2021; Yang et al. 2023) into FL can suffer from a significant challenge we refer to as *meta-information heterogeneity*, where summarizing data from non-IID distributions across clients can disrupt optimization and degrade performance. Without proper handling, such heterogeneity can deviate from the optimization direction, limiting the ability to reduce catastrophic forgetting effectively.

To address these challenges, we propose the Exemplar-Condensed federated class-incremental learning (ECoral) framework. ECoral enables the FL model to retain its performance on previously learned knowledge while incrementally learning new classes. It leverages a dual-distillation approach, where exemplars are distilled from the training dataset to capture more informative features, such as detailed contour information, enhanced texture, and richer color attributes, rather than relying on conventional sampling methods, as illustrated in Figure 1. Additionally, the model’s prior knowledge is distilled from the model trained on previous tasks, ensuring that new learning does not compromise previously acquired knowledge. The main contributions of this work can be summarized as follows:

- A clear definition of the meta-information heterogeneity problem in federated continual learning (FCL) is proposed, identifying it as a significant challenge that affects model performance across different data sources.
- A novel method called ECoral is proposed that features a dual-distillation structure specifically designed to address this issue by mitigating catastrophic forgetting in FCL.
- The proposed method in ECoral shifts from storing raw data to using condensed exemplars in memory, signifi-

cantly enhancing privacy protection by abstracting stored information into less recognizable forms and addressing key privacy concerns in federated learning.

- Extensive experiments validate the effectiveness of our proposed method. For instance, when the CIFAR-100 dataset is partitioned into ten tasks, our approach achieves an average accuracy of 49.17%, outperforming the best baseline by 5.32%. In a more challenging long-term continual learning scenario, where CIFAR-100 is divided into 50 tasks, our method reaches an average accuracy of 32.42%, surpassing the best baseline by 10.29%.

## Related Work

### Dataset Condensation

Dataset Condensation (DC) aims to reduce the size of a dataset while retaining enough representative information to allow machine learning models to perform comparably to training on the full dataset. Early works, such as those by Wang et al. (2018) and Zhao, Mopuri, and Bilen (2020), framed this as a bi-level optimization problem. The objective is to create a smaller, condensed dataset that preserves the original data’s characteristics, allowing a model trained on this smaller dataset to achieve high performance. These techniques often focus on matching distributions, features, or gradients between the original and condensed data. This concept has been successfully integrated into the field of continual learning, where DC methods help mitigate catastrophic forgetting by compressing the data of previous tasks into small but representative memory sets (Masarczyk and Tautkute 2020; Gu et al. 2024).

In the context of FL, several studies have explored the application of DC to reduce communication overhead by transmitting condensed datasets rather than full models or gradient updates between clients and the server (Goetz and Tewari 2020; Hu et al. 2022). For example, Liu, Yu, and Zhou (2022) employed DC to address the challenges posed by heterogeneous data in FL environments, reducing both communication costs and data bias. These efforts suggest that DC is well-suited for handling the resource constraints and privacy considerations inherent in FL, as synthetic data can be shared while preserving local client privacy. Our approach builds on these foundations by introducing DC into federated class-incremental learning (FCIL) to enhance the informativeness of memory exemplars and mitigate catastrophic forgetting in non-IID data scenarios.

### Federated Continual Learning

Federated Continual Learning (FCL) extends the traditional FL framework to dynamic environments, where new tasks or classes emerge incrementally over time. Unlike conventional FL, which assumes static data distributions, FCL must deal with continually evolving data and the challenges of catastrophic forgetting, non-IID data distribution, and communication constraints between clients and the server (Yoon et al. 2021).

To address catastrophic forgetting, one of the most common approaches in FCL is rehearsal-based methods. These

methods store a limited number of examples (exemplars) from previous tasks in memory and replay them to the model during training on new tasks, thereby helping to maintain the model’s knowledge of older classes (Dong et al. 2022; Qi, Zhao, and Li 2023). For instance, GLFC (Dong et al. 2022) employs sample reconstruction techniques to retain knowledge at the global level, while FedCIL (Qi, Zhao, and Li 2023) utilizes generative models to reconstruct past samples for rehearsal. Although effective in mitigating forgetting, these methods face significant challenges, especially in the context of federated settings where privacy and storage constraints are critical. TATGET (Zhang et al. 2023), an exemplar-free distillation method, offers a privacy-preserving alternative by leveraging knowledge distillation from previously trained global models. It uses a generator to produce synthetic data that simulates the global distribution, reducing the reliance on real data storage while addressing catastrophic forgetting in highly non-IID settings.

A major limitation of existing rehearsal-based methods is the issue of class imbalance at the exemplar memory level. Since most clients in FL do not possess data for all classes, the memory stored at each client is often biased towards the locally available classes. This imbalance exacerbates catastrophic forgetting during memory replay, as the model tends to overfit the classes that are well-represented in memory and underperform on underrepresented or unseen classes. Such imbalances are especially problematic in non-IID data settings, where the data distribution across clients can be highly skewed, further diminishing the effectiveness of memory replay. Even TARGET, despite its exemplar-free approach, relies on global knowledge distillation, which may struggle to capture the full diversity of class distributions across clients.

## Preliminaries

**Federated Class-incremental Learning.** Federated Class-incremental Learning (FCIL) aims to collaboratively train a global model using streaming data that sequentially introduces new classes. In this context, a model training process consists of a series of sequential tasks  $\mathcal{T} = \{\mathcal{T}^t\}_{t=1}^T$ , where  $T$  denotes the total number of tasks. The system involves  $C$  local clients and a central server  $S_g$ . Each task comprises  $R$  global communication rounds (where  $r = 1, \dots, R$ ), and in each round  $r$ , a subset of the local participants is randomly selected for gradient aggregation. When the  $l$ -th client  $C_l$  is selected for a given global round in the  $t$ -th incremental task, it receives the latest global model  $\theta^{r,t}$ .

Drawing inspiration from online learning, each client maintains a fixed-size local memory  $\mathcal{M}_l = \{(\mathbf{x}_{l,m}, \mathbf{y}_{l,m})\}_{m=1}^M$  of size  $M$ , storing examples from prior tasks for knowledge replay. In this work, we divide this memory into three parts:  $\mathcal{M}_{\text{orig}}$ , which holds original data sampled from the current task’s training set;  $\mathcal{M}_{\text{cond}}$ , which stores condensed exemplars from prior tasks; and  $\mathcal{M}_{\text{sum}}$ , which saves summarizing data from the current task. At each iteration of the current task, a batch of samples  $\mathbf{B}_m = \{(\mathbf{x}_{i,m}, \mathbf{y}^{i,m})\}_{i=1}^{B_m}$  is randomly drawn from the memory and jointly trained alongside the current task data

$\mathbf{B}_n = \{(\mathbf{x}_i^t, \mathbf{y}_i^t)\}_{i=1}^{B_n}$ . Here,  $B_m \leq M$  and  $B_n$  represent the mini-batch sizes of the replayed data and the current task data, respectively. The joint training objective is expressed as:

$$\theta_l^{r,t} = \arg \min_{\theta^{r,t}} \mathcal{L}(\theta^{r,t}; \mathbf{B}_n) + \lambda \mathcal{L}_m(\theta^{r,t}; \mathbf{B}_m), \quad (1)$$

where  $\mathcal{L}$  and  $\mathcal{L}_m$  are the loss functions for the current task data and memory data, respectively.  $\lambda$  is a hyper-parameter for regulation.

The client trains the global model  $\theta^{r,t}$  on its own  $t$ -th incremental task data  $\mathcal{D}_l^t \cup \mathcal{M}_l$ , where  $\mathcal{D}_l^t = \left\{ (\mathbf{x}_{l,i}^t, \mathbf{y}_{l,i}^t) \right\}_{i=1}^{N_l^t} \subset \mathcal{T}^t$  represents the training data for new categories specific to the  $l$ -th client. The category distribution for the  $l$ -th client is denoted by  $\mathbf{P}_l$ . The distributions  $\{\mathbf{P}_l\}_{l=1}^C$  are non-independent and identically distributed (non-IID). At the  $t$ -th incremental task, the label space  $\mathcal{Y}_l^t \subseteq \mathcal{Y}^t$  for the  $l$ -th local client is a subset of  $\mathcal{Y}^t = \bigcup_{l=1}^C \mathcal{Y}_l^t$ , which includes  $\mathcal{K}_l^t$  new categories ( $\mathcal{K}_l^t \leq \mathcal{K}^t$ ), distinct from the previous categories  $\mathcal{K}_l^p = \sum_{i=1}^{t-1} \mathcal{K}_l^i \subseteq \bigcup_{j=1}^{t-1} \mathcal{Y}_l^j$ . After receiving  $\theta^{r,t}$  and performing local training on the  $t$ -th incremental task, the  $l$ -th client obtains an updated model  $\theta_l^{r,t}$ . These locally updated models from selected clients are then uploaded to the central server  $S_g$ , where they are aggregated to form the new global model  $\theta^{r+1,t}$  for the next round. The central server  $S_g$  subsequently distributes the updated parameters  $\theta^{r+1,t}$  to the local clients for the following global round.

**Client increment strategy.** To better simulate a real-world federated continual learning application, we adopt the client increment strategy introduced in GLFC (Dong et al. 2022). This strategy divides local participants into three dynamic groups for each incremental task: Old ( $\mathcal{G}_o$ ), In-between ( $\mathcal{G}_b$ ), and New ( $\mathcal{G}_n$ ). The Old group ( $\mathcal{G}_o$ ), consisting of  $G_o$  participants, only has access to data from classes introduced in previous tasks and does not receive any data for the new task. The In-between group ( $\mathcal{G}_b$ ), with  $G_b$  members, works with both the new classes from the current task and the classes from the previous task. Finally, the New group ( $\mathcal{G}_n$ ), comprising  $G_n$  newly added participants, focuses exclusively on data containing new classes from the current task.

The group compositions are dynamically updated with the progression of tasks. Specifically, the membership of the groups  $\mathcal{G}_o, \mathcal{G}_b, \mathcal{G}_n$  is redefined randomly at each global round, and new participants are irregularly added to  $\mathcal{G}_n$  as incremental tasks arrive. This incremental process gradually increases the total number of participants,  $G = G_o + G_b + G_n$ , as more tasks are introduced, closely mimicking the nature of streaming data in real-world FL applications.

## Problem Definition

**Forgetting in FCIL** The primary objective of global model optimization at the  $t$ -th incremental task is to minimize the classification error across the current category set  $\mathcal{K}_t$ . However, when a new task arises, clients are often constrained by privacy restrictions and limited resources, allowing only restricted access to data from previous tasks. The

category imbalance between old and new categories ( $\mathcal{T}_l^t$  and  $\mathcal{M}_l$ ) at the local level exacerbates this issue, leading to significant performance degradation during local training. This limitation frequently results in a notable decline in performance on earlier tasks, a phenomenon known as catastrophic forgetting. To mitigate catastrophic forgetting in the global model, our goal is to minimize the classification error on the current category set  $\mathcal{K}_t$  while simultaneously preserving the knowledge of previously learned categories. The objective function is formally defined as:

$$\min_{\theta_t} \sum_{k \in \mathcal{K}_t} \sum_{i=1}^{N_k} \mathcal{L}(\mathbf{P}_l^t(\mathbf{x}_{l,i}^t; \theta_{r,t}), \mathbf{y}_{l,i}^t) \quad (2)$$

where  $\mathcal{L}$  is a loss function that measures the classification error, and  $N_k$  is the number of samples in class  $k$ .

**Meta-information Heterogeneity** The condensation of data from non-IID sources inherently retains the non-IID characteristics at an information level, leading to what we define as the meta-information heterogeneity problem. Given that each client’s original dataset  $\mathcal{D}_l^t$  on task  $t$ -th is drawn from a unique distribution  $\mathbf{P}_l(X, Y)$ , the resulting condensed exemplar dataset  $\mathcal{M}_{\text{cond}}$ , optimized to represent  $\mathcal{D}_l^t$ , will also reflect this distinct distribution. Mathematically, this is expressed as  $\mathbf{P}_l^{\text{cond}}(X, Y) \neq \mathbf{P}_{l'}^{\text{cond}}(X, Y)$  for some clients  $l \neq l'$ . The divergence in information content between these condensed datasets can be quantified using measures such as Kullback-Leibler (KL) divergence, where  $\text{KL}(\mathcal{I}(\mathcal{T}_l^{\text{cond}}) \parallel \mathcal{I}(\mathcal{T}_{l'}^{\text{cond}})) > 0$  indicates non-identical information content across clients, thus confirming meta-information heterogeneity. Non-IID data has been shown to exacerbate catastrophic forgetting, as explored in (Zhang et al. 2023), further complicating federated continual learning. Similarly, when these heterogeneous condensed datasets are used to train a global model  $\theta^{r,t}$ , the model’s updates from different clients may conflict due to the diverse information content, leading to suboptimal performance. This degradation is reflected in the global loss function  $\mathcal{L}(\theta)$ , which generally increases compared to an IID scenario, expressed as  $\Delta \mathcal{L} = \mathcal{L}_{\text{non-iid}}(\theta^{r,t}) - \mathcal{L}_{\text{iid}}(\theta^{r,t}) > 0$ . Therefore, condensed datasets from non-IID sources introduce a meta-information heterogeneity problem that adversely affects the global model’s performance, mirroring the challenges posed by non-IID data in traditional federated learning.

## Exemplar-condensed FCIL with Dual-distillation Structure

### Online Exemplars Condensation

In edge devices within FCIL, where memory space is highly restricted, most existing approaches focus on efficient exemplar sampling strategies. Compared to these, our approach enhances the meta-knowledge capacity of each individual image, thereby increasing its information level, and also balances these improvements with memory efficiency. The balance and trade-offs are further explained in the following sections, highlighting comparisons and improvements over existing methods.

**Adjustable Memory.** Efficiently managing a fixed memory space for rehearsal typically requires sophisticated selection algorithms that continually update stored examples, as proposed in methods like (Rebuffi et al. 2017; Aljundi et al. 2019). However, these approaches are not well-suited for our objective, which involves distilling meta-knowledge into exemplars from the entire local training dataset.

In contrast to conventional online learning methods like SSD (Gu et al. 2024), which employ a fixed exemplar position strategy for summarizing information, our approach addresses several key limitations. SSD assumes balanced class data in each batch and prior knowledge of the total number of classes, both of which are often unrealistic in real-world federated learning (FL) scenarios. Moreover, SSD allocates only a small fraction of memory to old exemplars. For instance, saving just one exemplar per class when training on a task with 100 total classes within a 100-exemplar space. This inefficient use of memory dedicates the majority of space to current data, hindering effective rehearsal. In an FL environment, this issue is further exacerbated by the non-IID nature of the data and class imbalance, as each client typically holds only a subset of the total class data. Additionally, in our scenario, since many clients do not participate in all tasks, SSD’s strategy often results in memory slots being predominantly occupied by current task data by the end of the whole training process.

To overcome these challenges, we propose a dynamic memory allocation strategy that adjusts the exemplar space by calculating the required number of samples for each class at the beginning of each task. This approach reduces the number of prior exemplars to free up space, ensuring balanced storage of prior task exemplars while incorporating current task data samples. For example, if the first task includes 10 classes and the total memory space is 100 exemplars, 10 samples are initially stored for each class. When the next task introduces 10 new classes, we reduce the number of exemplars for each previous class to 5 and allocate the remaining 50 slots to the new classes. This ensures a balanced distribution of memory across tasks and efficient rehearsal.

### Meta-knowledge Condensation via Gradient Matching.

In Federated Class Incremental Learning (FCIL), where each client is limited by constrained exemplar memory, our approach extends beyond simply managing exemplar selection. The aim is to enhance the information capacity of each image, thereby maximizing meta-knowledge to improve the effectiveness of rehearsal. The primary objective of Meta-Knowledge Condensation is to minimize the divergence between the memory set and the client’s local task  $\mathcal{T}_l$  training data distribution, resulting in an optimized memory set,  $\mathcal{M}_l$ . We hypothesize that the global model trained on exemplars with condensed meta-knowledge can perform similarly as it trained on the whole local training dataset in  $t$ -th task. Drawing inspiration from dataset condensation methods (Zhao, Mopuri, and Bilen 2020), the process is implemented by sequentially distilling knowledge from mini-batches of real data into summarized exemplars corresponding to each class.

Considering the  $t$ -th task, let the condensed exemplars for

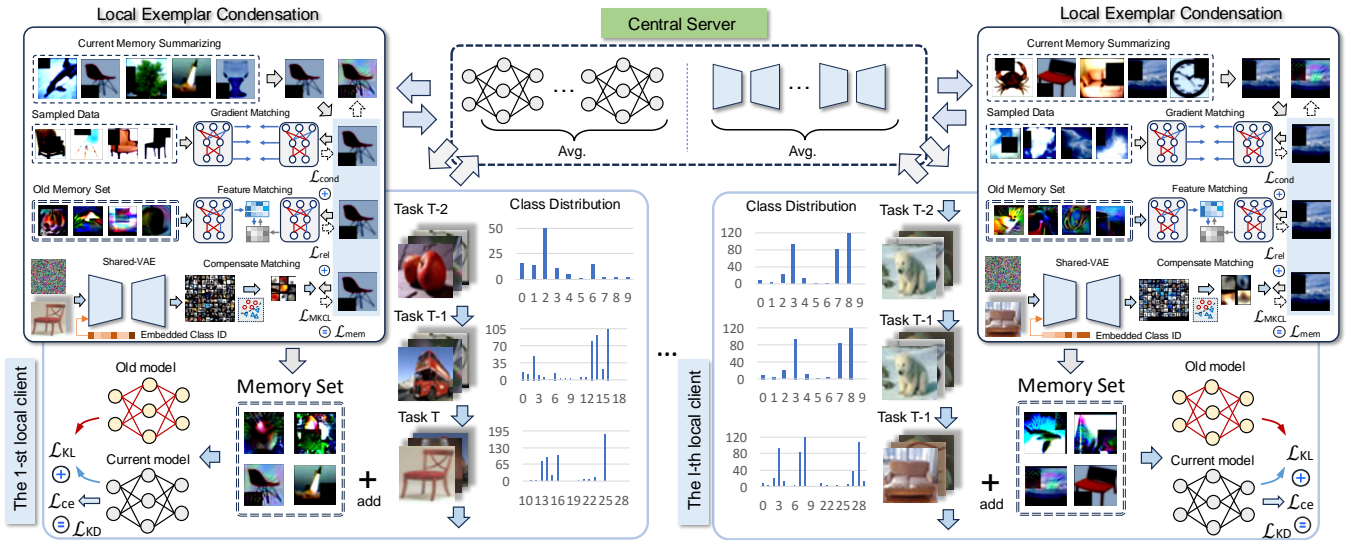


Figure 2: Overview of our ECoral framework. Clients (from the 1st to the  $l$ -th) continuously learn from new class data sequences, each using a dual-distillation structure to mitigate catastrophic forgetting during local training. The local exemplar condensation process involves three key components: a gradient matching loss ( $\mathcal{L}_{\text{cond}}$ ) to distill meta-information from the training dataset, a feature matching loss ( $\mathcal{L}_{\text{rel}}$ ) to ensure consistency between the mean features of condensed samples and real images, and a compensation matching loss ( $\mathcal{L}_{\text{MKCL}}$ ) to reduce the impact of meta-information heterogeneity problem, using disentangled features generated by a globally shared model (Shared-VAE). Additionally, a knowledge distillation loss ( $\mathcal{L}_{\text{KD}}$ ) helps the model retain previously learned knowledge.

a class  $k$  be denoted by  $\mathcal{M}_k$ , with a predefined size of  $m$ . The data points of the same class within the current mini-batch are represented by  $\mathbf{B}_k$ . The primary objective of the memory condensation process is to reduce the divergence between  $\mathcal{M}_k$  and  $\mathbf{B}_k$ . In the DC works by (Zhao, Mopuri, and Bilen 2020), a novel and efficient metric is introduced, which quantifies the distance between the gradients of the training process on the same neural network when comparing condensed samples with original data points. By aligning the gradient-based model update metrics across the stream of data, the condensed samples are progressively refined to approximate the training performance of the entire dataset. The objective function for gradient matching is defined as:

$$\mathcal{L}_{\text{cond}} = f_{\text{dist}}(\nabla_{\theta^{r,t}} \mathcal{L}_{\text{ce}}(\theta^{r,t}; \mathcal{M}_k), \nabla_{\theta^{r,t}} \mathcal{L}_{\text{ce}}(\theta^{r,t}; \mathbf{B}_k)) \quad (3)$$

, where  $f_{\text{dist}}$  is a distance function.

### Current Knowledge Condensation via Feature Matching.

In conventional dataset condensation (Zhao, Mopuri, and Bilen 2020), gradient matching is often alternated with model updates. The primary goal is to simulate a comprehensive training process that allows for the matching of gradients across various training stages. During each training iteration, when a new batch of stream data  $\mathbf{B}_n$  is introduced, the parameters  $\omega$  of the condensation model are first randomly initialized and updated as follows:

$$\omega \leftarrow \omega - \eta \nabla_{\omega} \mathcal{L}_{\text{ce}}(\omega; \mathbf{B}_n), \quad (4)$$

where  $\eta$  is the learning rate for the condensation model, at this stage, only real images participate in the model summarization update, which prevents knowledge leakage from the summarized samples.

However, in the context of continual learning, the number of classes is not fixed throughout the training process. To address this challenge, we draw inspiration from the SSD approach (Gu et al. 2024), which suggests re-initializing the model when new classes are introduced. To prevent the loss of valuable gradient information when the model's decision boundaries are constructed only for current classes, we employ dataset condensation across multiple dataset batches. This approach updates the model using both current stream data and stored real images in memory  $\mathcal{M}_{\text{orig}}$ :

$$\omega \leftarrow \omega - \eta \nabla_{\omega} (\mathcal{L}_{\text{ce}}(\omega; \mathbf{B}_n) + \mathcal{L}_{\text{ce}}(\omega; \mathcal{M}_{\text{orig}})) \quad (5)$$

Building on the SSD approach, a relationship-matching strategy is implemented to further refine the condensation process. By using the extracted features of previously summarized samples as anchors, consistency is explicitly enforced between the mean features of condensed samples and real images, ensuring they maintain a consistent relationship with these anchors. The objective for relationship matching is defined as:

$$\mathcal{L}_{\text{rel}} = f_{\text{dist}}(\rho(\mathcal{M}_k, \mathcal{M}_{\text{cond}} \setminus \mathcal{M}_k, \omega), \rho(\mathbf{B}_k, \mathcal{M}_{\text{cond}} \setminus \mathcal{M}_k, \omega))$$

$$\rho(\mathcal{X}_1, \mathcal{X}_2, \omega) = f_{\text{dist}}\left(\frac{1}{|\mathcal{X}_1|} \sum_{x \in \mathcal{X}_1} \Phi(\omega; x), \Phi(\omega; \mathcal{X}_2)\right) \quad (6)$$

, where  $\rho$  represents the relationship calculation,  $\mathcal{M}_{\text{cond}} \setminus \mathcal{M}_k$  refers to the condensed samples excluding  $\mathcal{M}_k$ ,  $\Phi$  de-

notes the feature extraction function. This relationship consistency helps establish a more balanced distribution of condensed samples within the memory.

As defined in Section , the condensed exemplars from non-iid data can still leave the meta-information heterogeneous, which affects replay efficiency. Thus, this problem must be addressed from both data quantity shift and class shift problems in a privacy-preserving way.

**Client-wise Feature Disentanglement.** To address the feature and class skew problem, our goal is to enable each client not only to extract and generate features from the local dataset but also to generate features that are not visible in the local data but present in other clients’ datasets, such as color, structure, and texture characteristics. By generating these features from random noise for classes unseen locally but present in other clients, the label skew problem can be reduced. The disentanglement approach (Burgess et al. 2018; Higgins et al. 2017) is an efficient method for low-level feature extraction. As previously discussed, the heterogeneity of meta-knowledge arises from two main issues: feature skew and class skew. To tackle both challenges, we proposed the Client-wise Shared Conditional Variational Auto-Encoder (Shared-VAE) model. In this model, both the encoder  $E_\phi(x) = q_\phi(z|x)$  and the decoder  $D_\theta(z) = p_\theta(x|z)$  are updated through FL in each round. This allows the encoder to improve its ability to extract and refine hidden latent based on global knowledge while the decoder generates information that extends beyond the local data distribution by leveraging local latent information. At the beginning of the local model update, both the local encoder  $E_\phi^l$  and decoder  $D_\theta^l$  of the  $l$ -th client are updated with the latest global parameters  $E_\phi^g$  and  $D_\theta^g$ , respectively. The local training dataset is then directly used to generate a set of disentangled features if the class data is available locally, addressing the feature skew problem. Otherwise, for classes unseen locally, features are generated from random noise to address the label skew problem. The class ID is provided as a condition during feature generation, ensuring that the model generates class-specific features. The resulting feature set is represented as  $\mathbf{H}$ . After each round of local model updates, the Shared-VAE model is further refined using only the local training data.

**Unbiased Representative Feature Prototypes** However, a globally updated Shared-VAE tends to generate features that predominantly represent the majority distribution across all clients. For example, while most cats have fur, a smaller subset, like the Sphynx cat, do not. As a result, when these representations are used to guide data condensation, the condensed data may become biased towards this majority distribution, leading to skewed optimization. To address this limitation, we propose the use of unbiased representative feature prototypes. Specifically, each class  $k$  can be represented by multiple characteristic features, denoted as  $\mathbf{H}_k = \{\mathbf{h}_i \mid y_i = k\}$ , where  $y_i$  is the class label for feature  $\mathbf{h}_i$ . These features are grouped using an unsupervised clustering method, FINCH (Sarraz, Sharma, and Stiefelagen 2019), which is parameter-free and suitable for scenarios where the number

of clients is uncertain.

First, the data are divided into groups by category, with one group of data for each class, denoted as  $G_k$  for class  $k$ . Then, FINCH is applied to cluster each group  $G_k$  to extract characteristic features for each class. After applying FINCH clustering, each group  $G_k$  is divided into  $V_k$  clusters, represented as  $\mathcal{Q}_k = \{\mathcal{Q}_{k,j}\}_{j=1}^{V_k}$ , where  $\mathcal{Q}_{k,j}$  represents the  $j$ -th cluster for class  $k$ . Next, the average of all feature vectors in each cluster is directly computed to obtain the representative feature prototype for that cluster:

$$\mathbf{u}_{k,j} = \frac{1}{|\mathcal{Q}_{k,j}|} \sum_{\mathbf{h}_i \in \mathcal{Q}_{k,j}} \mathbf{h}_i \quad (7)$$

Here,  $\mathbf{u}_{k,j}$  is the prototype for cluster  $j$  in class  $k$ , calculated by averaging all the features  $\mathbf{h}_i$  within that cluster. Each class  $k$  is represented by the set of prototypes from all its clusters:

$$\mathbf{U}_k = \{\mathbf{u}_{k,j}\}_{j=1}^{V_k} \quad (8)$$

Finally, the overall set of representative prototypes for all classes is given by:

$$\mathcal{U} = \{\mathbf{U}_k\}_{k=1}^C \quad (9)$$

This ensures that each class  $k$  is represented by the averaged prototypes of its clusters, providing a balanced and representative set of features for further processing.

**Meta-knowledge Compensate Matching.** By incorporating more class-specific characteristic features in the condensed exemplars while minimizing class-irrelevant features, we hypothesize that more discriminative representations can be created, resulting in clearer decision boundaries between different classes. To achieve this, for the current task’s condensed data  $\mathcal{M}_{\text{cond}}$ , we ensure that the condensed data is similar to its corresponding class prototypes  $\mathcal{P}^k$ , and dissimilar to prototypes of other classes, represented as  $\mathcal{N}^k = \bar{\mathbf{U}} - \mathcal{P}^k$ .

The similarity between the embedding of a query sample  $\mathbf{z}_i$  and the corresponding cluster prototypes  $\mathbf{u} \in \bar{\mathbf{U}}$  is calculated using cosine similarity. For two feature vectors  $\mathbf{z}_i$  and  $\mathbf{u}$ , the cosine similarity is defined as:

$$\text{sim}(\mathbf{z}_i, \mathbf{u}) = \frac{\mathbf{z}_i \cdot \mathbf{u}}{\|\mathbf{z}_i\| \times \|\mathbf{u}\|/\tau} \quad (10)$$

where  $\mathbf{z}_i = f(x_i)$  is the embedding of sample  $x_i$ , and  $\tau$  is a temperature parameter that controls sensitivity to similarities.

Therefore, the aim is to optimize the characters of each data sample to bring the local features of the current class closer to the global set of features for that class while distancing them from the characters of other classes. This optimization is intended to maintain a clear decision boundary, allowing the model to perform replay efficiently. By doing so, the feature distribution of this class can remain balanced across all clients in FL at the level of the character. Thus, we propose Meta-knowledge Contrastive Learning (MKCL) for compensating matching, which contrasts cluster prototypes of the same class for each query sample against those

of other classes with differing semantics. This approach naturally results in the following optimization objective term:

$$\mathcal{L}_{\text{MKCL}} = -\log \frac{\sum_{\mathbf{u} \in \mathcal{P}^k} \mathbb{E}(\text{sim}(\mathbf{z}_i, \mathbf{u}))}{\sum_{\mathbf{u} \in \mathcal{P}^k} \mathbb{E}(\text{sim}(\mathbf{z}_i, c)) + \sum_{\mathbf{u} \in \mathcal{N}^k} \mathbb{E}(\text{sim}(\mathbf{z}_i, \mathbf{u}))} \quad (11)$$

, finally, we can define as

$$\log \left( \sum_{\mathbf{u} \in \mathcal{N}^k} \mathbb{E}(\text{sim}(\mathbf{z}_i, \mathbf{u})) \right) - \log \left( \sum_{\mathbf{u} \in \mathcal{P}^k} \mathbb{E}(\text{sim}(\mathbf{z}_i, \mathbf{u})) \right) \quad (12)$$

Here, we can summarise the total objective of exemplar condensation as follows:

$$\mathcal{L}_{\text{mem}} = \mathcal{L}_{\text{cond}} + \mathcal{L}_{\text{rel}} + \beta \mathcal{L}_{\text{MKCL}}, \quad (13)$$

where  $\beta$  is weighting coefficients for meta-knowledge contrastive learning.

### Prior Knowledge Supervision.

Another important part of the dual-distillation structure is knowledge distillation, which is used to transfer knowledge from previous tasks to new tasks, thereby mitigating the problem of catastrophic forgetting. We directly implement Knowledge Distillation (Rebuffi et al. 2017; Li and Hoiem 2017; Wu et al. 2019) widely used in continual learning, which aims to leverage the soft output of a previously trained global model (named teacher model) as a regularization term for the training of the current task global model (named student model).

Mathematically, let  $p_{t-1}(x)$  denote the probability distribution (softmax output) of the teacher model after training on the previous task  $t-1$ , and  $p_t(x)$  denote the distribution of the student model being trained on the current task  $t$ . The goal is to minimize the following objective function:

$$\mathcal{L}_{\text{KD}} = \mathcal{L}_{\text{ce}} + \lambda \cdot \mathcal{L}_{\text{KL}} \quad (14)$$

, where  $\mathcal{L}_{\text{KL}} = KL(p_{t-1}(x) \parallel p_t(x))$

Here,  $\mathcal{L}_{\text{ce}}$  represents the task-specific cross-entropy loss for the current task  $t$ , such as cross-entropy loss, and  $\mathcal{L}_{\text{KL}}$  is the loss function of Kullback-Leibler divergence  $KL(p_{t-1}(x) \parallel p_t(x))$  between the teacher’s and student’s output distributions, which serves as the distillation loss. The parameter  $\lambda$  controls the balance between the task loss and the distillation loss. By minimizing this objective, the student model learns to perform well on the new task while retaining knowledge from previous tasks, thus reducing catastrophic forgetting.

## Experimental Setup

### Implementation details.

In this work, all methods were implemented using PyTorch (Paszke et al. 2019) and executed on a single NVIDIA RTX 4090 GPU paired with an AMD 7950X CPU, utilizing ResNet18 (He et al. 2016) as the backbone for feature extraction in our classification models. The FedAvg algorithm (McMahan et al. 2017) was employed for global

model aggregation. Each task involved training the model over  $R = 50$  communication rounds, with each client performing  $E = 30$  local epochs per round. A learning rate of 0.003 was used across all datasets to achieve optimal performance, and Stochastic Gradient Descent (SGD) served as the optimizer in all experiments. Unless specified otherwise, the constraint factor  $\lambda$  in the Elastic Weight Consolidation (EWC) method was set to 300. For knowledge distillation, the temperature parameter was set to 2, and the distillation loss weight  $\lambda$  was set to 3. And based on our experimental results and a thorough grid search, we set  $\beta = 0.5$  for all experiments. To simulate non-IID data distributions, we partitioned the datasets among clients using the Latent Dirichlet Allocation (LDA) method, where the concentration parameter  $\sigma$  controls the degree of data skew; we varied  $\sigma$  to simulate different levels of non-IID data. For experiments on the CIFAR-100 and TinyImageNet datasets, we started with 20 clients and selected 10 clients per round, incrementing the total number of clients by 5 with each new task for the CIFAR-100 experiments with 10 and 20 tasks. However, due to data quantity limitations, only 1 client was incremented per new task in the 50-task CIFAR-100 experiment. Conversely, for the Caltech256 dataset, due to the limited number of samples per class, we started with 5 clients, selected 50% of the total clients in each round, and incremented the total number of clients by 1 with each new task. In all experiments, for each new task, 90% of the existing clients  $\mathcal{U}_o$  transitioned to the new task. To clearly illustrate the data distributions across clients under varying degrees of non-IID settings (controlled by  $\sigma$ ), Figure 3 presents the data distribution for the final task in the CIFAR-100 dataset experiment with a total of 10 tasks. A further detailed breakdown of the data distribution across all clients for each task is illustrated in Fig 3.

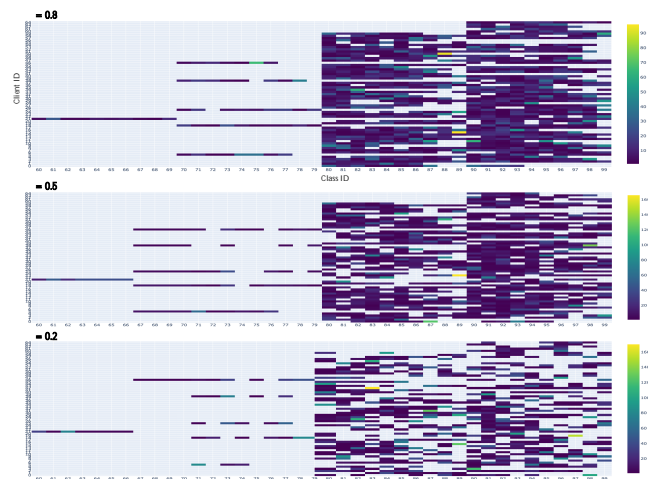


Figure 3: Training data distribution of every client for CIFAR-100 on the final task, with non-IID levels  $\sigma$  of 0.2, 0.5, and 0.8 across a total of 10 tasks (each task containing 10 classes).

## Datasets

We evaluated the framework on three widely used datasets for image classification tasks: CIFAR-100, TinyImageNet, and Caltech-256. The CIFAR-100 dataset (Krizhevsky, Hinton et al. 2009) consists of 60,000 color images of size  $32 \times 32$  pixels, distributed across 100 classes with 600 images per class. We allocated an exemplar memory space of 100 for each client and partitioned the dataset into tasks of varying sizes: 10 tasks with 10 classes per task, 20 tasks with 5 classes per task, and 50 tasks with 2 classes per task. The TinyImageNet dataset (Le and Yang 2015) contains 100,000 images of size  $64 \times 64$  pixels, distributed over 200 classes with 500 images per class. We allocated an exemplar memory space of 200 for each client and evaluated our method using 10 tasks, each comprising 20 classes. The Caltech-256 dataset (Griffin et al. 2007) includes 30,607 images across 257 classes; we removed the “background” class, originally used for validation, resulting in a total of 256 classes. Each image was resized to  $64 \times 64$  pixels due to computational resource constraints. We allocated an exemplar memory space of 256 for each client and evaluated our method using 16 tasks with 16 classes per task.

## Baselines

**Replay** maintains an exemplar memory at each client to store and replay a subset of previous data, mitigating catastrophic forgetting in federated learning settings by randomly selecting samples from the training data and incrementally adding new classes with each new task.

**iCaRL** (Rebuffi et al. 2017) proposes an incremental learning method that integrates representation learning with a nearest-mean-of-exemplars classifier, utilizing a fixed memory budget to store exemplars from previous classes, thereby mitigating catastrophic forgetting while learning new classes.

**LwF** (Li and Hoiem 2017) enables a neural network to learn new tasks without forgetting previously learned tasks by using knowledge distillation to preserve the model’s responses on old tasks during training, all without requiring access to the original data from the old tasks.

**EWC** (Kirkpatrick et al. 2017) mitigates catastrophic forgetting in neural networks by adding a regularization term that penalizes changes to important weights, identified using the Fisher information matrix. This approach allows the model to learn new tasks while preserving performance on previously learned tasks without requiring access to old data.

**BiC** (Wu et al. 2019) tackles the bias toward new classes in class-incremental learning by introducing a two-stage training framework that adds a bias correction layer, which is fine-tuned using a small validation set to adjust the decision boundary between old and new classes, effectively reducing bias and improving classification accuracy.

**TARGET** (Zhang et al. 2023) addresses federated class-continual learning by introducing an exemplar-free distillation method that utilizes global prototypes to preserve knowledge of previous classes without storing or generating data, effectively mitigating catastrophic forgetting in a privacy-preserving manner.

**FedCIL** (Qi, Zhao, and Li 2023) addresses federated class-incremental learning by introducing a global knowledge distillation method to preserve knowledge of old classes and a class-balanced sampling strategy to mitigate class imbalance, enabling clients to learn new classes while reducing catastrophic forgetting incrementally.

## Evaluation Metrics

**Accuracy ( $\mathcal{A}$ )**: This metric computes the accuracy for a given task. We report the final accuracy after all tasks have been trained as  $\mathcal{A}_{last}$ , and the average accuracy across the last round of every task as  $\mathcal{A}_{avg}$ .

**Averaged Incremental Accuracy  $\mathcal{A}^{inc}$**  (Rebuffi et al. 2017): This metric calculates the average accuracy after the completion of each task, emphasizing the model’s performance throughout the incremental learning process. We denote the overall averaged accuracy across all tasks as  $\mathcal{A}_{avg}^{inc}$ , and the accuracy after the last task as  $\mathcal{A}_{last}^{inc}$ .

**Accuracy A ( $\mathcal{A}^a$ )** (Díaz-Rodríguez et al. 2018): As defined by Díaz-Rodríguez et al., this metric differs from standard accuracy by assigning equal weight to the accuracy of each task, regardless of the number of samples. For instance, in a scenario where Task 1 has 50,000 images and Task 2 has 1,000 images, standard accuracy would give more weight to Task 1, whereas Accuracy A treats both tasks equally. We denote the overall averaged Accuracy A as  $\mathcal{A}_{avg}^a$  and the Accuracy A after the last task as  $\mathcal{A}_{last}^a$ .

**Backward Transfer (BwT)** (Lopez-Paz and Ranzato 2017): This metric measures the influence that learning a new task has on the performance of previously learned tasks. A positive BwT indicates an improvement in past tasks after learning new ones, while a negative BwT signifies forgetting. It is denoted as BwT.

**Forward Transfer (FwT)** (Lopez-Paz and Ranzato 2017): This metric assesses the influence that learning a new task has on the performance of future tasks. Positive forward transfer implies that learning prior tasks benefits future tasks, enhancing initial performance. It is denoted as FwT.

**Remembering** (Díaz-Rodríguez et al. 2018): This metric calculates the degree of retention for previous tasks as part of the backward transfer process. It quantifies how well the model remembers earlier tasks after learning new ones.

**Forgetting** (Chaudhry et al. 2018): This metric measures the average amount of forgetting across all tasks, helping to quantify how much information is lost as new tasks are learned. It is calculated by comparing the maximum performance on a task with its performance after learning subsequent tasks.

## Results

**ECoral efficiently mitigates forgetting.** As shown in Table 1 with  $\sigma = 0.5$ , and extended further in Table 2 with more complex datasets, ECoral consistently outperforms other baseline methods across multiple evaluation metrics. For the CIFAR-100 dataset at  $\sigma = 0.5$ , ECoral achieves an impressive average accuracy ( $\mathcal{A}_{avg}$ ) of 49.17% and a last-task accuracy ( $\mathcal{A}_{last}$ ) of 27.97%, significantly surpassing iCaRL, the closest baseline, which only reaches an  $\mathcal{A}_{avg}$



of 43.85% and  $\mathcal{A}_{last}$  of 21.76%. This underscores ECoral’s superior ability to mitigate catastrophic forgetting and maintain strong performance across tasks compared to other methods.

When examining more complex datasets like Tiny-ImageNet and Caltech-256, ECoral continues to demonstrate its effectiveness. On Tiny-ImageNet, ECoral achieves the best average accuracy ( $\mathcal{A}_{avg}$  of 38.78%), outperforming iCaRL, which records 36.46%. Though iCaRL slightly surpasses ECoral in last-task accuracy ( $\mathcal{A}_{last}$  22.80% vs. 20.88%), ECoral’s overall performance balance across tasks highlights its ability to manage incremental learning effectively. A similar trend is seen with the Caltech-256 dataset, where ECoral achieves the highest average accuracy ( $\mathcal{A}_{avg}$  of 31.06%) but slightly trails iCaRL in last-task accuracy (21.66% vs. 23.52%). This small gap in last-task accuracy can be explained by iCaRL’s emphasis on incremental learning for recent tasks, whereas ECoral focuses on holistic task balance, trading off minor performance losses on the last task for superior average accuracy across all tasks.

Despite these few instances where iCaRL outperforms ECoral in last-task accuracy, ECoral consistently excels in overall task performance, demonstrating its strength in mitigating forgetting across all tasks. These results highlight ECoral as an effective approach for continual learning, particularly in scenarios where sustained performance across many tasks is critical.

**ECoral balance the knowledge learned in each task.** As illustrated in Figure 4, the CIFAR-100 experiments with  $\sigma = 0.5$  provide a detailed analysis of ECoral’s performance as tasks are progressively introduced, reflecting a typical continual learning scenario. In the early stage, for the first task (T0), all methods show strong performance, with Target and iCaRL slightly outperforming ECoral in the initial steps. Nonetheless, ECoral remains highly competitive, demonstrating a robust ability to learn and adapt right from the start.

As additional tasks are introduced (from T1 to T9), the common challenge of catastrophic forgetting becomes more evident, with all methods experiencing a gradual decline in performance. ECoral, however, distinguishes itself by maintaining a more stable and balanced performance compared to baselines like BiC, FedCIL, and Replay, which show more pronounced declines as tasks are added. ECoral’s ability to sustain balanced performance across tasks allows it to mitigate forgetting more effectively, maintaining competitive results even as the complexity of the continual learning setting increases.

In the later stages (T8 and T9), while ECoral is occasionally outperformed by Target and iCaRL in last-task accuracy, this is primarily due to the incremental learning emphasis of those methods, which prioritize performance on recent tasks. However, ECoral’s superior average accuracy across all tasks underscores its strength in balancing performance over the entire task sequence. This approach ensures that ECoral not only excels in the earlier tasks but also performs well across a wide range of tasks, making it more resilient to the long-term challenges of catastrophic forgetting.

Overall, the results demonstrate ECoral’s effectiveness in

preserving knowledge across multiple tasks, delivering superior stability and resilience compared to other baseline methods under the CIFAR-100 dataset with  $\sigma = 0.5$ .

**ECoral is keep effective at different levels of non-iid.** The experimental results, shown in Table 1, assessed using three key metrics: Accuracy ( $\mathcal{A}$ ), Averaged Incremental Accuracy ( $\mathcal{A}^{incree}$ ), and Accuracy A ( $\mathcal{A}^a$ ), highlight the strong performance of ECoral compared to baseline methods across various non-IID data distributions. ECoral consistently shows higher final accuracy ( $\mathcal{A}_{last}$ ) and average accuracy ( $\mathcal{A}_{avg}$ ) across all tasks, particularly excelling in more challenging non-IID settings such as  $\sigma = 0.2$ , which represents the most highly skewed data scenario. In this difficult setting, ECoral demonstrates robustness by effectively retaining knowledge from previous tasks and adapting to new ones, significantly reducing catastrophic forgetting. For instance, at  $\sigma = 0.2$ , ECoral shows marked improvements in both  $\mathcal{A}_{last}$  and  $\mathcal{A}_{avg}$  compared to other methods. Furthermore, ECoral performs exceptionally well in Averaged Incremental Accuracy ( $\mathcal{A}^{incree}$ ), maintaining higher accuracy throughout the incremental learning process. Even as the non-IID severity decreases (e.g.,  $\sigma = 0.5$  and  $\sigma = 0.8$ ), ECoral continues to outperform competing approaches, demonstrating adaptability across different levels of data skew. Additionally, ECoral achieves high scores in Accuracy A ( $\mathcal{A}^a$ ), which balances performance across tasks irrespective of sample size. Notably, even in the highly skewed  $\sigma = 0.2$  scenario, ECoral achieves an  $\mathcal{A}_{avg}^a$  of 49.58%, outperforming the next best method by a significant margin, further underscoring its robustness and fairness across tasks. Overall, these results confirm ECoral’s effectiveness in mitigating catastrophic forgetting and improving task performance in federated continual learning, especially in environments with highly non-IID data distributions.

**ECoral achieves superior performance across multiple evaluation metrics.** Beyond its strong accuracy, as illustrated in Figure 5, ECoral also excels across other important metrics such as Backward Transfer (BwT), Forward Transfer (FwT), Forgetting, and Remembering. ECoral shows lower negative BwT compared to several baseline methods, managing to limit the detrimental effects on previously learned tasks as new tasks are introduced. While iCaRL and Target demonstrate slightly better backward transfer in earlier stages, ECoral avoids the significant negative transfer experienced by methods like FedCIL and BiC, which exhibit steep performance declines when more tasks are added. This demonstrates that ECoral effectively preserves prior knowledge, a key requirement for successful continual learning.

Moreover, ECoral displays strong forward transfer (FwT), suggesting that learning earlier tasks contributes positively to the performance on future tasks. This is especially important in non-IID settings where task distributions may vary significantly. Compared to FedCIL and BiC, which struggle with forward transfer, ECoral leverages knowledge from earlier tasks to improve initial performance on new tasks. Additionally, ECoral demonstrates significantly lower forgetting, particularly in the later stages of task learning, indicating that it retains information long-term and resists the catastrophic forgetting seen in methods like FedCIL and BiC.

Table 1: Results on CIFAR100 with 10 tasks with non-IID levels  $\sigma$  of 0.2, 0.5, and 0.8 across a total of 10 tasks (each task containing 10 classes), evaluated across three metrics:  $\mathcal{A}$ ,  $\mathcal{A}^{incre}$ , and  $\mathcal{A}^a$  for both the last task and overall performance.  $\Delta$  represents the absolute difference compared to the results of our ECoral method.

The results row of our ECoral is highlighted in  . Improvements are marked in green, and declines are marked in red.

Methods	$\sigma = 0.2$				$\sigma = 0.5$				$\sigma = 0.8$			
	$\mathcal{A}_{avg}$	$\Delta$	$\mathcal{A}_{last}$	$\Delta$	$\mathcal{A}_{avg}$	$\Delta$	$\mathcal{A}_{last}$	$\Delta$	$\mathcal{A}_{avg}$	$\Delta$	$\mathcal{A}_{last}$	$\Delta$
Replay	32.82	10.70	16.63	12.09	36.72	12.45	18.72	9.25	37.49	11.85	18.05	13.34
iCaRL	31.97	11.55	20.46	8.26	43.85	5.32	21.76	6.21	44.97	4.37	23.58	7.81
EWC	31.73	11.79	14.03	14.69	36.55	12.62	16.56	11.41	38.59	10.75	18.42	12.97
BiC	28.27	15.25	13.08	15.64	33.45	15.72	17.49	10.48	35.62	13.72	16.31	15.08
LwF	36.64	6.88	16.93	11.79	43.13	6.04	21.38	6.59	44.69	4.65	22.90	8.49
TARGET	30.60	12.92	9.42	19.30	41.51	7.66	16.71	11.26	46.05	3.29	20.83	10.56
FedCIL	30.14	13.38	13.62	15.10	34.88	14.29	15.56	12.41	34.98	14.36	16.05	15.34
ECoral	43.52	–	28.72	–	49.17	–	27.97	–	49.34	–	31.39	–

Methods	$\mathcal{A}_{avg}^{incre}$		$\mathcal{A}_{last}^{incre}$		$\mathcal{A}_{avg}^{incre}$		$\mathcal{A}_{last}^{incre}$		$\mathcal{A}_{avg}^{incre}$		$\mathcal{A}_{last}^{incre}$	
	$\mathcal{A}_{avg}^{incre}$	$\Delta$	$\mathcal{A}_{last}^{incre}$	$\Delta$	$\mathcal{A}_{avg}^{incre}$	$\Delta$	$\mathcal{A}_{last}^{incre}$	$\Delta$	$\mathcal{A}_{avg}^{incre}$	$\Delta$	$\mathcal{A}_{last}^{incre}$	$\Delta$
Replay	45.35	7.61	36.72	12.45	51.01	9.48	32.82	10.70	52.88	7.01	37.49	11.85
iCaRL	46.45	6.51	43.85	5.32	57.37	3.12	36.20	7.32	57.43	2.46	44.97	4.37
EWC	46.32	6.64	36.55	12.62	52.54	7.95	31.73	11.79	55.35	4.54	38.59	10.75
BiC	41.57	11.39	33.45	15.72	48.99	11.50	28.27	15.25	51.33	8.56	35.62	13.72
LwF	49.25	3.71	43.13	6.04	57.18	3.31	36.64	6.88	59.89	–	44.69	4.65
TARGET	45.50	7.46	41.51	7.66	57.47	3.02	30.60	12.92	61.42	1.53	46.05	3.29
FedCIL	44.25	8.71	34.88	14.29	49.84	10.65	30.14	13.38	50.92	8.97	34.98	14.36
ECoral	52.96	–	49.17	–	60.49	–	43.52	–	59.89	–	49.34	–

Methods	$\mathcal{A}_{avg}^a$		$\mathcal{A}_{last}^a$		$\mathcal{A}_{avg}^a$		$\mathcal{A}_{last}^a$		$\mathcal{A}_{avg}^a$		$\mathcal{A}_{last}^a$	
	$\mathcal{A}_{avg}^a$	$\Delta$	$\mathcal{A}_{last}^a$	$\Delta$	$\mathcal{A}_{avg}^a$	$\Delta$	$\mathcal{A}_{last}^a$	$\Delta$	$\mathcal{A}_{avg}^a$	$\Delta$	$\mathcal{A}_{last}^a$	$\Delta$
Replay	40.39	9.19	28.23	13.74	45.22	11.16	25.26	12.20	46.66	9.47	28.31	14.25
iCaRL	42.68	6.90	35.33	6.64	52.37	4.01	29.71	7.75	52.97	3.16	36.97	5.59
EWC	40.27	9.31	27.02	14.95	46.09	10.29	23.19	14.27	48.53	7.60	28.65	13.91
BiC	36.02	13.56	24.46	17.51	42.44	13.94	20.52	16.94	44.87	11.26	26.36	16.20
LwF	44.25	5.33	34.40	7.57	51.85	4.53	29.03	8.43	54.06	2.07	35.32	7.24
TARGET	39.65	9.93	31.13	10.84	51.88	4.50	21.54	15.92	55.98	0.15	36.12	6.44
FedCIL	38.43	11.15	25.84	16.13	43.91	12.47	21.84	15.62	44.35	11.78	25.60	16.96
ECoral	49.58	–	41.97	–	56.38	–	37.46	–	56.13	–	42.56	–

In terms of Remembering, ECoral shows competitive performance, ensuring that it retains knowledge of previously learned tasks effectively. While iCaRL slightly outperforms ECoral in specific cases, ECoral’s overall balance between retention, forward transfer, and reduced forgetting ensures it can handle the trade-offs inherent in continual learning, providing robust long-term performance across multiple tasks.

**ECoral can perform consistently in a long-term training task.** The results shown in Figure 6 demonstrate that ECoral significantly outperforms baseline methods in both 20-task and 50-task continual learning setups, particularly in terms of average and final accuracy. In the 20-task setup, ECoral consistently maintains higher average accuracy compared to competing methods, achieving 63.60% for the average accuracy across tasks, while methods such as BiC (51.4%) and Replay (55.27%) fall behind. By the final task, ECoral still retains a strong accuracy of 59.00%, whereas BiC (39.6%) and FedCIL (38.25%) exhibit substantial declines. In the more challenging 50-task setup, ECoral continues to lead, with an average accuracy of 91.00%, outperforming

BiC (90.50%) and iCaRL (90.00%). As the number of tasks increases, ECoral maintains a notable performance edge, with a final accuracy of 64.40% by the last task, significantly higher than BiC (36.90%) and Replay (38.40%). These results highlight ECoral’s superior ability to retain knowledge and perform consistently across both short- and long-term continual learning setups, emphasizing its robustness and scalability in federated learning environments.

**ECoral is user privacy friendly.** This work addresses user privacy concerns in two key areas. First, we ensure that the Shared-VAE model cannot regenerate raw data from other clients and that the generated data is not semantically interpretable by humans, preserving data privacy at the federated learning (FL) level. Second, we design the condensed data to be recognizable only as belonging to the client’s local classes, yet indecipherable by humans, to prevent privacy breaches during memory replay.

To illustrate this, Figure 7 displays six randomly selected samples of disentangled features generated by Shared-VAE alongside six condensed exemplars. As seen in the left panel,

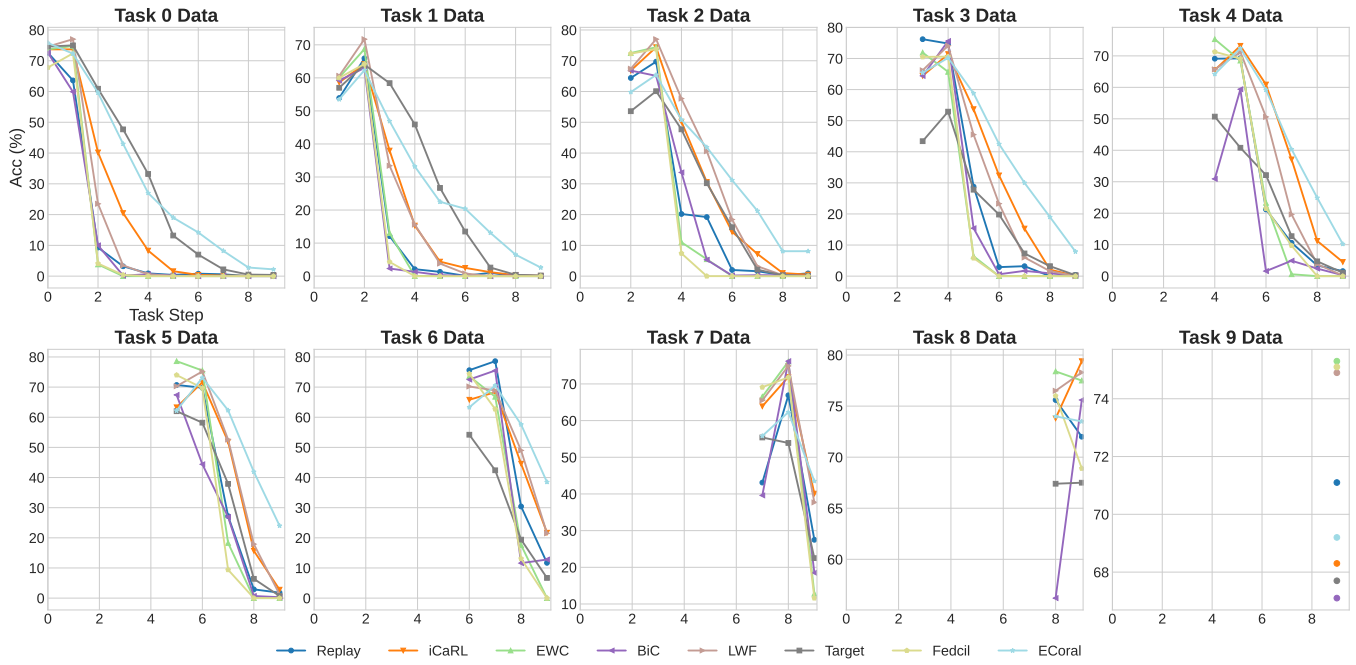


Figure 4: Performance evaluation on CIFAR100 under a Non-IID setting with  $\sigma = 0.5$ , across 10 tasks. The final accuracy  $\mathcal{A}$  (%) for each learned task is reported after the completion of each task.

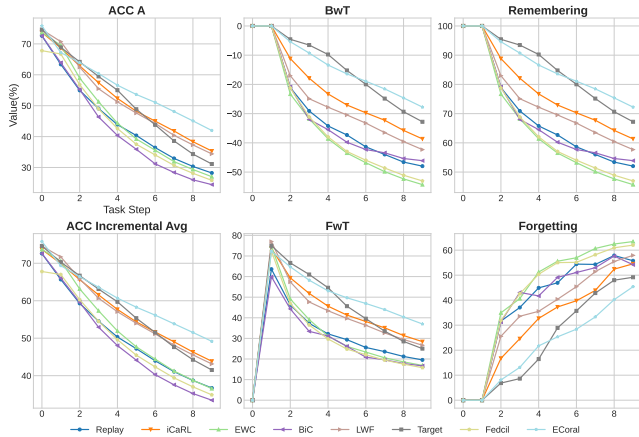


Figure 5: Evaluation of multiple metrics (%) on CIFAR100 under a Non-IID setting with  $\sigma = 0.5$ , across a total of 10 tasks.

the disentangled features are highly abstract, containing only basic information such as colors and vague outlines, rendering them indistinguishable to humans. In the right panel, even though the first row of condensed exemplars can be roughly associated with a certain category, the details remain unclear, ensuring that no specific class details from client data are exposed. Importantly, these condensed exemplars are derived solely from the user’s local training data without incorporating any sensitive information from other clients. The second row of exemplars is entirely unrecognizable, further enhancing in-memory data-level privacy protection.

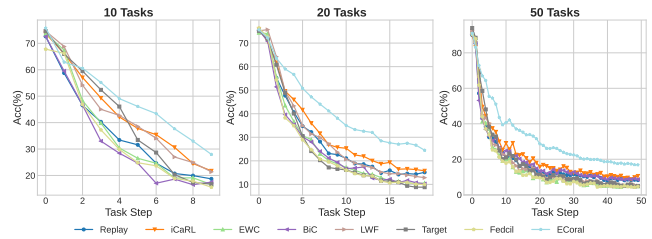


Figure 6: Performance evaluation on CIFAR100 under a Non-IID setting with  $\sigma = 0.5$ . The final accuracy  $\mathcal{A}$  (%) is reported after learning each task. The left plot shows results with 10 steps (10 classes per task), the middle with 20 steps (5 classes per task), and the right with 50 steps (2 classes per task).

## Conclusion

In this paper, we propose the ECoral framework, which successfully addresses critical challenges in Federated Class-Incremental Learning (FCIL) by enhancing memory efficiency and improving resilience against catastrophic forgetting. The combination of exemplar condensation and meta-knowledge contrastive learning allows the model to store more informative and privacy-preserving condensed exemplars, while client-wise feature disentanglement mitigates the negative effects of data heterogeneity. This approach ensures consistent performance across highly non-IID environments, making it well-suited for real-world federated learning applications where data privacy and resource constraints are key concerns. However, we observe that ECoral’s advantage decreases when applied to more complex datasets. Fu-

Table 2: Results on Tiny-ImageNet with 10 tasks (10 classes per task) and on Caltech-256 with 16 tasks (16 classes per task), both under a Non-IID setting with  $\sigma = 0.5$ .

The results row of our ECoral is highlighted in  . The best result is highlighted with  , and the second-best result is highlighted with  .

Methods	Tiny-Imagenet (10 Tasks)						Caltech-256 (16 Tasks)					
	$\mathcal{A}_{avg}$	$\mathcal{A}_{last}$	$\mathcal{A}_{avg}^{incre}$	$\mathcal{A}_{last}^{incre}$	$\mathcal{A}_{avg}^a$	$\mathcal{A}_{last}^a$	$\mathcal{A}_{avg}$	$\mathcal{A}_{last}$	$\mathcal{A}_{avg}^{incre}$	$\mathcal{A}_{last}^{incre}$	$\mathcal{A}_{avg}^a$	$\mathcal{A}_{last}^a$
Replay	35.73	18.73	46.04	33.51	41.72	26.17	24.24	20.92	31.46	24.24	28.20	20.79
iCaRL	<span style="background-color: #ffe0e0;">36.46</span>	<span style="background-color: #ffe0e0;">22.80</span>	44.92	<span style="background-color: #ffe0e0;">35.40</span>	41.56	<span style="background-color: #ffe0e0;">29.69</span>	26.72	<span style="background-color: #ffe0e0;">23.52</span>	33.75	26.72	30.54	23.11
EWC	31.10	13.10	45.23	30.14	39.19	21.49	20.68	11.08	34.17	20.68	28.12	13.67
BiC	35.88	20.46	46.31	34.51	42.07	27.57	<span style="background-color: #ffe0e0;">29.26</span>	<span style="background-color: #ffe0e0;">22.70</span>	<span style="background-color: #ffe0e0;">37.78</span>	<span style="background-color: #ffe0e0;">29.26</span>	<span style="background-color: #ffe0e0;">33.84</span>	<span style="background-color: #ffe0e0;">24.51</span>
LwF	35.76	16.78	<span style="background-color: #ffe0e0;">47.51</span>	33.64	<span style="background-color: #ffe0e0;">42.53</span>	25.54	23.20	12.88	35.51	23.20	30.06	16.67
TARGET	27.00	10.49	40.83	25.46	34.63	16.90	20.46	10.31	35.28	20.46	27.83	12.15
FedCIL	30.18	12.59	44.67	29.11	38.43	20.13	18.53	10.53	31.16	18.53	25.59	11.92
<span style="background-color: #e0e0ff;">ECoral</span>	<span style="background-color: #ffe0e0;">38.78</span>	<span style="background-color: #ffe0e0;">20.88</span>	<span style="background-color: #ffe0e0;">48.46</span>	<span style="background-color: #ffe0e0;">37.80</span>	<span style="background-color: #ffe0e0;">44.94</span>	<span style="background-color: #ffe0e0;">31.24</span>	<span style="background-color: #e0e0ff;">31.06</span>	<span style="background-color: #e0e0ff;">21.66</span>	<span style="background-color: #ffe0e0;">40.64</span>	<span style="background-color: #ffe0e0;">31.06</span>	<span style="background-color: #ffe0e0;">36.23</span>	<span style="background-color: #ffe0e0;">25.11</span>

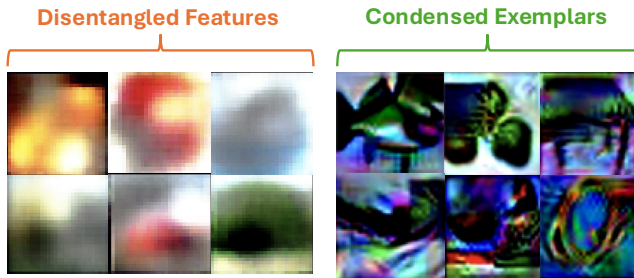


Figure 7: Examples of disentangled features from Shared-VAE and final condensed exemplars.

ture work will focus on strengthening ECoral’s performance in these complex scenarios, ensuring robustness and scalability across diverse real-world data challenges.

## References

Aljundi, R.; Lin, M.; Goujaud, B.; and Bengio, Y. 2019. Gradient based sample selection for online continual learning. *Advances in neural information processing systems*, 32.

Burgess, C. P.; Higgins, I.; Pal, A.; Matthey, L.; Watters, N.; Desjardins, G.; and Lerchner, A. 2018. Understanding disentangling in  $\beta$ -VAE. *arXiv preprint arXiv:1804.03599*.

Cazenavette, G.; Wang, T.; Torralba, A.; Efros, A. A.; and Zhu, J.-Y. 2022. Dataset distillation by matching training trajectories. In *Proceedings of the IEEE/CVF Conference on Computer Vision and Pattern Recognition*, 4750–4759.

Chaudhry, A.; Dokania, P. K.; Ajanthan, T.; and Torr, P. H. 2018. Riemannian walk for incremental learning: Understanding forgetting and intransigence. In *Proceedings of the European conference on computer vision (ECCV)*, 532–547.

Díaz-Rodríguez, N.; Lomonaco, V.; Filliat, D.; and Maltoni, D. 2018. Don’t forget, there is more than forgetting: new metrics for Continual Learning. *arXiv preprint arXiv:1810.13166*.

Dong, J.; Li, H.; Cong, Y.; Sun, G.; Zhang, Y.; and Van Gool, L. 2024. No One Left Behind: Real-World Federated Class-

Incremental Learning. *IEEE Transactions on Pattern Analysis and Machine Intelligence*, 46(4): 2054–2070.

Dong, J.; Wang, L.; Fang, Z.; Sun, G.; Xu, S.; Wang, X.; and Zhu, Q. 2022. Federated class-incremental learning. In *Proceedings of the IEEE/CVF Conference on Computer Vision and Pattern Recognition*, 10164–10173.

Goetz, J.; and Tewari, A. 2020. Federated learning via synthetic data. *arXiv preprint arXiv:2008.04489*.

Griffin, G.; Holub, A.; Perona, P.; et al. 2007. Caltech-256 object category dataset. Technical report, Technical Report 7694, California Institute of Technology Pasadena.

Gu, J.; Wang, K.; Jiang, W.; and You, Y. 2024. Summarizing Stream Data for Memory-Constrained Online Continual Learning. In *Proceedings of the AAAI Conference on Artificial Intelligence*, volume 38, 12217–12225.

He, K.; Zhang, X.; Ren, S.; and Sun, J. 2016. Deep residual learning for image recognition. In *Proceedings of the IEEE conference on computer vision and pattern recognition*, 770–778.

Higgins, I.; Matthey, L.; Pal, A.; Burgess, C. P.; Glorot, X.; Botvinick, M. M.; Mohamed, S.; and Lerchner, A. 2017. beta-vae: Learning basic visual concepts with a constrained variational framework. *ICLR (Poster)*, 3.

Hu, S.; Goetz, J.; Malik, K.; Zhan, H.; Liu, Z.; and Liu, Y. 2022. Fedsynth: Gradient compression via synthetic data in federated learning. *arXiv preprint arXiv:2204.01273*.

Jiang, Y.; Ma, B.; Wang, X.; Yu, G.; Yu, P.; Wang, Z.; Ni, W.; and Liu, R. P. 2024. Blockchained federated learning for internet of things: A comprehensive survey. *ACM Computing Surveys*, 56(10): 1–37.

Kirkpatrick, J.; Pascanu, R.; Rabinowitz, N.; Veness, J.; Desjardins, G.; Rusu, A. A.; Milan, K.; Quan, J.; Ramalho, T.; Grabska-Barwinska, A.; et al. 2017. Overcoming catastrophic forgetting in neural networks. *Proceedings of the national academy of sciences*, 114(13): 3521–3526.

Krizhevsky, A.; Hinton, G.; et al. 2009. Learning multiple layers of features from tiny images.

- Le, Y.; and Yang, X. 2015. Tiny imagenet visual recognition challenge. *CS 231N*, 7(7): 3.
- Li, Z.; and Hoiem, D. 2017. Learning without forgetting. *IEEE transactions on pattern analysis and machine intelligence*, 40(12): 2935–2947.
- Liu, P.; Yu, X.; and Zhou, J. T. 2022. Meta knowledge condensation for federated learning. *arXiv preprint arXiv:2209.14851*.
- Lopez-Paz, D.; and Ranzato, M. 2017. Gradient episodic memory for continual learning. *Advances in neural information processing systems*, 30.
- Ma, Y.; Xie, Z.; Wang, J.; Chen, K.; and Shou, L. 2022. Continual federated learning based on knowledge distillation. In *Proceedings of the Thirty-First International Joint Conference on Artificial Intelligence*, volume 3.
- Masarczyk, W.; and Tautkute, I. 2020. Reducing catastrophic forgetting with learning on synthetic data. In *Proceedings of the IEEE/CVF Conference on Computer Vision and Pattern Recognition Workshops*, 252–253.
- McMahan, B.; Moore, E.; Ramage, D.; Hampson, S.; and y Arcas, B. A. 2017. Communication-efficient learning of deep networks from decentralized data. In *Artificial intelligence and statistics*, 1273–1282. PMLR.
- Nguyen, D. C.; Ding, M.; Pathirana, P. N.; Seneviratne, A.; Li, J.; and Poor, H. V. 2021. Federated learning for internet of things: A comprehensive survey. *IEEE Communications Surveys & Tutorials*, 23(3): 1622–1658.
- Nguyen, D. C.; Pham, Q.-V.; Pathirana, P. N.; Ding, M.; Seneviratne, A.; Lin, Z.; Dobre, O.; and Hwang, W.-J. 2022. Federated learning for smart healthcare: A survey. *ACM Computing Surveys (Csur)*, 55(3): 1–37.
- Paszke, A.; Gross, S.; Massa, F.; Lerer, A.; Bradbury, J.; Chanan, G.; Killeen, T.; Lin, Z.; Gimelshein, N.; Antiga, L.; et al. 2019. Pytorch: An imperative style, high-performance deep learning library. *Advances in neural information processing systems*, 32.
- Qi, D.; Zhao, H.; and Li, S. 2023. Better generative replay for continual federated learning. *arXiv preprint arXiv:2302.13001*.
- Rebuffi, S.-A.; Kolesnikov, A.; Sperl, G.; and Lampert, C. H. 2017. icarl: Incremental classifier and representation learning. In *Proceedings of the IEEE conference on Computer Vision and Pattern Recognition*, 2001–2010.
- Rosasco, A.; Carta, A.; Cossu, A.; Lomonaco, V.; and Bacciu, D. 2021. Distilled replay: Overcoming forgetting through synthetic samples. In *International Workshop on Continual Semi-Supervised Learning*, 104–117. Springer.
- Sarfraz, S.; Sharma, V.; and Stiefelwagen, R. 2019. Efficient parameter-free clustering using first neighbor relations. In *Proceedings of the IEEE/CVF conference on computer vision and pattern recognition*, 8934–8943.
- Wang, K.; Zhao, B.; Peng, X.; Zhu, Z.; Yang, S.; Wang, S.; Huang, G.; Bilen, H.; Wang, X.; and You, Y. 2022. Cafe: Learning to condense dataset by aligning features. In *Proceedings of the IEEE/CVF Conference on Computer Vision and Pattern Recognition*, 12196–12205.
- Wang, T.; Zhu, J.-Y.; Torralba, A.; and Efros, A. A. 2018. Dataset distillation. *arXiv preprint arXiv:1811.10959*.
- Wu, Y.; Chen, Y.; Wang, L.; Ye, Y.; Liu, Z.; Guo, Y.; and Fu, Y. 2019. Large scale incremental learning. In *Proceedings of the IEEE/CVF conference on computer vision and pattern recognition*, 374–382.
- Xiong, Y.; Wang, R.; Cheng, M.; Yu, F.; and Hsieh, C.-J. 2023. Feddm: Iterative distribution matching for communication-efficient federated learning. In *Proceedings of the IEEE/CVF Conference on Computer Vision and Pattern Recognition*, 16323–16332.
- Yang, E.; Shen, L.; Wang, Z.; Liu, T.; and Guo, G. 2023. An efficient dataset condensation plugin and its application to continual learning. *Advances in Neural Information Processing Systems*, 36.
- Yoon, J.; Jeong, W.; Lee, G.; Yang, E.; and Hwang, S. J. 2021. Federated continual learning with weighted inter-client transfer. In *International Conference on Machine Learning*, 12073–12086. PMLR.
- Zhang, J.; Chen, C.; Zhuang, W.; and Lyu, L. 2023. Target: Federated class-continual learning via exemplar-free distillation. In *Proceedings of the IEEE/CVF International Conference on Computer Vision*, 4782–4793.
- Zhao, B.; and Bilen, H. 2023. Dataset condensation with distribution matching. In *Proceedings of the IEEE/CVF Winter Conference on Applications of Computer Vision*, 6514–6523.
- Zhao, B.; Mopuri, K. R.; and Bilen, H. 2020. Dataset condensation with gradient matching. *arXiv preprint arXiv:2006.05929*.